

Uniaxial anisotropy of organic thin films determined by ellipsometry

U. Heinemeyer^{*1}, A. Hinderhofer¹, M. I. Alonso², J. O. Ossó^{2,3}, M. Garriga², M. Kytka^{1,4}, A. Gerlach¹, and F. Schreiber¹

¹ Institut für Angewandte Physik, Auf der Morgenstelle 10, 72076 Tübingen, Germany

² Institut de Ciència de Materials de Barcelona – CSIC Esfera UAB, 08193 Bellaterra, Barcelona, Spain

³ MATGAS 2000 A.I.E., Esfera UAB, 08193 Bellaterra, Barcelona, Spain

⁴ Faculty of Electrical Engineering and Information Technology, Slovak University of Technology, Ilkovicova 3, 81219 Bratislava, Slovakia

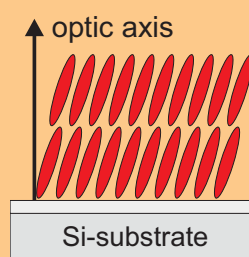
Received 8 June 2007, revised 29 December 2007, accepted 22 January 2008

Published online 26 March 2008

PACS 78.20.Ci, 78.66.Qn

* Corresponding author: e-mail ute.heinemeyer@uni-tuebingen.de, Phone: +49-07071-2976333, Fax: +49-07071-295110

Organic thin films frequently exhibit strong anisotropic optical constants, which in many cases are uniaxial with the optic axis oriented along the surface normal. The data analysis presented here to obtain the anisotropic optical constants of thin films on silicon substrates is based on the model system diindenoperylene (DIP), but nevertheless applies to all uniaxial films on SiO₂. In addition to variable angle spectroscopic ellipsometry, different substrates are used to perform a multiple sample analysis. This way of analysing data increases the sensitivity to uniaxial anisotropy.



© 2008 WILEY-VCH Verlag GmbH & Co. KGaA, Weinheim

1 Introduction Ellipsometry is a powerful tool to determine optical properties of thin films that are relevant for the fundamental understanding of condensed matter as well as for applications [1, 2]. Organic materials like small organic molecules or long chain polymers have received increased attention in thin film applications due to their promising and novel characteristics, such as flexibility and the enormous diversity to tailor specific properties [3]. One of the major differences to inorganic semiconductors is the increased orientational degree of freedom for organic molecules since they exhibit specific shapes, which significantly influences the film growth. Associated with this, crystalline organic thin films frequently have strongly anisotropic optical properties [4, 5]. In the case of isotropic substrates such as SiO₂ there will be no preferred in-plane direction, thus leading to uniaxial symmetry of the organic

film with the optic axis oriented parallel to the surface normal. The data analysis presented here is based on the model system diindenoperylene (DIP) (see inset of Fig. 2) on SiO₂. However, this paper concentrates on quite general technical issues concerning uniaxial geometry. A further discussion of the obtained optical properties of DIP thin films including electronic structure calculations is beyond the scope of this paper and will be published elsewhere [6]. Results based on the same data analysis procedure were obtained also for pentacene and perfluoropentacene thin films and are reported elsewhere [7].

From the literature it is known that variable angle spectroscopic ellipsometry (VASE) is not very sensitive to uniaxial anisotropy on native oxide [8–10]. Therefore, it was proposed to use thick thermal oxide as a substrate, in order to decorrelate the optical constants of the in-plane and of

the out-of-plane component [8]. The major drawback of this method is the potentially strong influence of uncertainties in the optical constants of the thermal oxide. Therefore, results obtained by this method are compared to a second approach, where transmission ellipsometry is combined with reflection ellipsometry which is also known to decouple the different components [11].

2 Experimental The DIP films were grown by organic molecular beam deposition (OMBD, see e.g. [12, 13]) at a substrate temperature of $T = 130\text{ °C}$ and a rate of 4 Å/min in ultrahigh vacuum with a base pressure of $2 \times 10^{-10}\text{ mbar}$. Three different substrates were used: silicon with native oxide, silicon with a 146 nm thick thermal oxide and a glass substrate. Before growth all three substrates were cleaned in an ultrasonic bath with acetone and isopropanol and finally rinsed with purified water. While X-ray data confirm that the film crystal structure on the different substrates can be considered identical, there are some morphological differences. A detailed discussion is beyond the scope of the present work, but these differences do not have a strong influence on the optical anisotropy. In the following the DIP film on native oxide will be referred to as $\text{DIP-Si}_{\text{Native}}$ and the films on thermal oxide as $\text{DIP-Si}_{\text{ThOx}}$ and on glass as DIP-Glass , respectively. In order to perform the multiple sample analyses and to couple film thicknesses in the fit, $\text{DIP-Si}_{\text{Native}}$ was always grown simultaneously with either $\text{DIP-Si}_{\text{ThOx}}$ or DIP-Glass . A film thickness of $(33 \pm 1.5)\text{ nm}$ was chosen for all samples to achieve the highest possible sensitivity for anisotropy and to keep roughness effects small, both effects increasing with film thickness. Furthermore, it is known that under the above described growth conditions and in this thickness range DIP crystallizes in a single so-called σ -phase where the molecules are standing nearly upright [14].

After growth variable angle ellipsometry data were measured ex-situ for each sample with a commercial spectroscopic ellipsometer (Woollam M2000) in the wavelength range of 245–980 nm with a spectral resolution of $\sim 1.59\text{ nm}$. The angle of incidence was varied between 45° and 80° in steps of 5° with an accuracy of 0.05° . In case of the glass substrate additional transmission ellipsometry data were measured with the same instrument and the angle of incidence was changed between 0° and 50° in steps of 10° with an accuracy of 0.5° .

3 Results and discussion

3.1 Data analysis The models for the substrates were determined prior to the film growth by using the commercial WVASE32 software. The optical constants of Si and native oxide were taken from the database [15], whereas the dielectric constant of the thermal oxide and the glass substrate were measured separately. They could be well described by a Cauchy function for the glass substrate (fixed thickness of 0.5 mm) and a Sellmeier-equation for the thermal oxide, which was fitted simultaneously with

the oxide thickness (146 nm) and an interfacial layer (1.5 nm [15]).

The DIP film thickness on $\text{Si}_{\text{Native}}$ was determined by X-ray reflectometry because the thickness analysis of the ellipsometry data alone does not give unambiguous results. Moreover, it is essentially impossible to determine a film thickness by ellipsometry on top of a glass substrate due to similar refractive indices [16], the DIP-Glass thickness was assumed to be equal to the $\text{DIP-Si}_{\text{Native}}$ thickness. The same applies for $\text{DIP-Si}_{\text{ThOx}}$ since already small deviations of the thermal oxide's optical constant and thickness lead to strong deviations in the DIP film thickness, which therefore cannot be determined accurately.

The optical constants of the DIP film above the band gap are fitted in the region of 410–620 nm, where the uniaxial anisotropy has to be taken into account. Generally, an isotropic fit approach will not give the average properties of both axes [9] but will produce artificial absorption features [17]. Figure 1 shows the ellipsometry data Ψ of the $\text{DIP-Si}_{\text{ThOx}}$ film for three different angles of incidence (AOI). Furthermore the fit results are plotted for an isotropic fit which was performed at $\text{AOI} = 65^\circ$. While this isotropic fit describes the data well at $\text{AOI} = 65^\circ$, coinciding nearly with the data, significant differences are visible below 500 nm at $\text{AOI} = 45^\circ, 80^\circ$, which indicates that an isotropic model is not sufficient to describe the data [18]. Therefore the DIP film is described by using different in-plane and out-of-plane components. The absorption in these components can be described by analytical functions based on, e.g., Gaussian oscillators. Since the analytical fit depends on the choice of initial parameters, it is necessary to first perform a so-called point-by-point fit where the set of four optical constants (real and imaginary part for in-plane and out-of-plane component respectively) is fitted at each wavelength separately. As is known from the literature [8], it is very difficult if not impossible to extract these four constants unambiguously from VASE data for a single $\text{Si}_{\text{Native}}$ substrate.

Three different point-by-point-fits are performed in order to extract the uniaxial optical constants of the DIP film. First, the $\text{DIP-Si}_{\text{Native}}$ film is fitted separately which is referred to as the ' $\text{Si}_{\text{Native}}$ fit'. Second, a multiple sample analysis is performed using the $\text{DIP-Si}_{\text{Native}}$ and $\text{DIP-Si}_{\text{ThOx}}$ film that were grown simultaneously and it is referred to as the ' $\text{Si}_{\text{Native}} + \text{Si}_{\text{ThOx}}$ fit'. Third, another multiple sample analysis is performed using the $\text{DIP-Si}_{\text{Native}}$ film and the transmission and reflection ellipsometry data of the DIP-Glass film which is referred to as the ' $\text{Si}_{\text{Native}} + \text{Glass}$ fit'. In both multiple sample analyses the thickness as well as the optical constants of the films are coupled to be the same. Furthermore, the back reflection for the glass substrate has to be included in the model when performing the ' $\text{Si}_{\text{Native}} + \text{Glass}$ fit'. Two different algorithms were used to perform the point-by-point fits to exclude algorithm problems in the fitting procedures. The Woollam software and our own β -scan program code [19] produced the same results. The good agreement between the ellipsometry

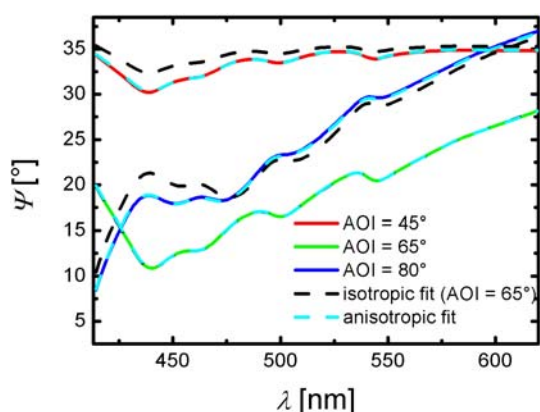


Figure 1 (online colour at: www.pss-a.com) Ellipsometry data Ψ of the DIP film on thermal oxide versus wavelength for different angles of incidence (AOI). The isotropic fit, obtained for AOI = 65° differs significantly from the data at other AOI's below 500 nm, whereas the anisotropic multiple sample fit ('Si_{Native} + Si_{ThOx} fit') agrees well.

data and the uniaxial fits are shown in Fig. 1 for the 'Si_{Native} + Si_{ThOx} fit' representatively.

3.2 Fit results The imaginary part ε_2 of the dielectric constant obtained from both multiple sample fits is plotted in Fig. 2a for the in-plane component and Fig. 2b for the out-of-plane component, whereas the real part ε_1 (Kramers Kronig consistent) is not depicted. Since the 'Si_{Native} fit' does not give reasonable results, although it describes the ellipsometry data well, it is not shown here. The 'Si_{Native} + Si_{ThOx} fit' and the 'Si_{Native} + Gl fit' lead to similar optical constants in both components, although there are some differences. While the in-plane components differ mostly below 500 nm the out-of-plane component shows a more similar line shape but with slightly different absolute values. Additionally, the 'Si_{Native} + Gl fit' exhibits absorption above 600 nm, where the DIP-film is expected to be transparent. We tried to eliminate such apparent absorption by including an additional EMA-layer and fitting at

slightly different thicknesses, but the result was qualitative independent of these parameters. Furthermore, we want to point out that the fit on the thermal oxide works also without the additional native oxide, giving similar though not the same results, whereas the glass data alone do not give unambiguous results.

In order to distinguish the best fit for describing the DIP film the first step is to compare the mean square error (MSE) between the fits. Since it is problematic to compare absolute MSE values between different measurements due to systematic errors [20], only MSE-values of different models applied to the same data set can be compared in order to distinguish the best fit. While the 'Si_{Native} fit' does not describe the DIP-Glass and DIP-Si_{ThOx} data, the 'Si_{Native} + Glass fit' and the 'Si_{Native} + Si_{ThOx} fit' describe the single DIP-Si_{Native} data well, although the 'Si_{Native} fit' itself works better. The still good agreement of the multiple sample fits to the DIP-Si_{Native} data indicates limited sensitivity of the data, which is the reason for unphysical optical constants, whereas the thermal oxide as well as additional transmission data decorrelate the fit parameters. This decorrelation effect can be demonstrated by comparing the correlation matrix for the different fits. The correlation coefficient (defined by $S_{ij} = C_{ij} / \sqrt{C_{ii}C_{jj}}$ with C_{ij} being an element of the covariance matrix [20]) between the in-plane and the out-of-plane component of ε_2 is plotted in Fig. 3 for all three fitting procedures. $|S_{ij}|$ is significantly smaller for the 'Si_{Native} + Si_{ThOx} fit' than for the 'Si_{Native} fit' in the entire energy range. The same holds for the 'Si_{Native} + Glass fit' below 560 nm. Above 560 nm $|S_{ij}|$ is even higher compared to the 'Si_{Native} fit'. The other correlation coefficients are not depicted here since they show similar behaviour. The correlation between the in-plane and the out-of-plane component for DIP-Si_{Native} cannot be reduced by using, e.g., Gaussian oscillators for describing the dielectric constant. This correlation does not depend on the model but solely on the experimental data that are used. When performing the multiple sample analysis, the results from the point-by-point fits presented here agree well with an additional Gaussian fit.

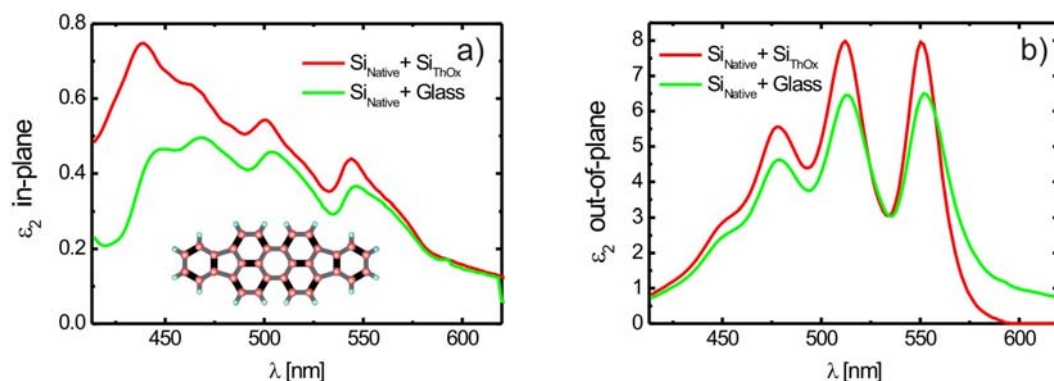


Figure 2 (online colour at: www.pss-a.com) Imaginary part ε_2 of the dielectric constant plotted for different point-by-point fit procedures (see text): a) in-plane component, b) out-of-plane component.

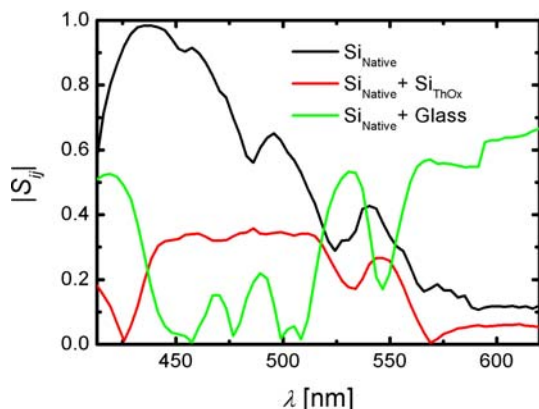


Figure 3 (online colour at: www.pss-a.com) Correlation coefficient $|S_{ij}|$ between the in-plane and the out-of-plane component of ϵ_2 at different wavelengths for different fitting procedures.

Both multiple sample fits are therefore more reliable to determine the optical constants of the DIP film and the ‘Si_{Native} fit’ gives an incorrect result. It is surprising, however, that the optical spectra could be reproduced very well for different DIP-Si_{Native} films then. The differences between the multiple sample fits may be due to systematic errors such as back reflection on the DIP-Glass film and different film morphology between DIP-Glass and DIP-Si_{Native}, which we observed by AFM measurements. Furthermore, scattering could be the origin of the offset in the out-of-plane component of the ‘Si_{Native}+Gl fit’, which is not included by the model. Therefore and since the correlation coefficients for the ‘Si_{Native} + Si_{ThOx} fit’ are smaller than those of the ‘Si_{Native} + Gl fit’ (in the transparent range), the ‘Si_{Native} + Si_{ThOx} fit’ gives the more reliable result for the optical constants of DIP thin films on silicon oxide.

4 Conclusion We have shown that the uniaxial optical constants of organic thin films, in this case DIP, can be obtained by performing a multiple sample fit using VASE data of two films on different substrates. One substrate is silicon with native oxide, while the other is either a 146 nm thick thermal oxide or glass. It is necessary to include one of the additional substrates in order to obtain reliable optical constants, because a fit on the native oxide does not give reasonable results due to parameter correlation. In case of the thermal oxide it is not necessary to include the native oxide data whereas the fit with the glass data works only when including the native oxide data. The multiple sample fits have significant lower correlation coefficients and they agree among each other although there appear

also differences. Since there are some uncertainties concerning the glass fit the thermal oxide fit is believed to be more reliable.

Acknowledgements Financial support by the EPSRC and the University of Tübingen is gratefully acknowledged. Helpful discussions with R. Scholz and R. Jacobs are gratefully acknowledged.

References

- [1] D. E. Aspnes, *Thin Solid Films* **89**, 249 (1982).
- [2] J. T. Zettler, *Prog. Cryst. Growth Charact.* **35**, 27 (1997).
- [3] W. K. Tommie, P. F. Baude, C. Gerlach, D. E. Ender, D. Muyres, M. A. Haase, D. E. Vogel, and S. D. Theiss, *Chem. Mater.* **16**, 4413 (2004).
- [4] M. Schubert, C. Bundesmann, G. Jakopic, H. Maresch, H. Arwin, N. C. Persson, F. Zhang, and O. Inganäs, *Thin Solid Films* **455/456**, 295 (2004).
- [5] M. Schubert, C. Bundesmann, G. Jakopi, H. Maresch, and H. Arwin, *Appl. Phys. Lett.* **84**, 200 (2004).
- [6] U. Heinemeyer, R. Scholz, L. Gisslén, J. O. Ossó, M. I. Alonso, M. Garriga, S. Kowarik, A. Gerlach, and F. Schreiber, to be published.
- [7] A. Hinderhofer, U. Heinemeyer, A. Gerlach, S. Kowarik, R. M. J. Jacobs, Y. Sakamoto, T. Suzuki, and F. Schreiber, *J. Chem. Phys.* **127**, 194705 (2007).
- [8] E. G. Bortchagovsky, *Thin Solid Films* **307**, 192 (1997).
- [9] D. J. D. Smet, *J. Appl. Phys.* **76**, 2571 (1994).
- [10] M. Campoy-Quiles, P. G. Etchegoin, and D. D. C. Bradley, *Phys. Rev. B* **72**, 045209 (2005).
- [11] C. M. Ramsdale and N. C. Greenham, *Adv. Mater.* **14**, 212 (2002).
- [12] G. Witte and C. Wöll, *J. Mater. Res.* **19**, 1889 (2004).
- [13] F. Schreiber, *phys. stat. sol. (a)* **201**, 1037 (2004).
- [14] S. Kowarik, A. Gerlach, S. Sellner, F. Schreiber, L. Cavalcanti, and O. Konovalov, *Phys. Rev. Lett.* **96**, 125504 (2006).
- [15] C. M. Herzinger, B. Johs, W. A. McGahan, J. A. Woollam, and W. Paulson, *J. Appl. Phys.* **83**, 3323 (1998).
- [16] H. G. Tompkins, T. Tiwald, C. Bungay, and A. E. Hooper, *J. Vac. Sci. Technol. A* **24**, 1605 (2006).
- [17] M. J. Dignam, M. Moskovits, and R. W. Stobie, *Trans. Faraday Soc.* **67**, 3306 (1971).
- [18] M. Schubert, B. Rheinländer, E. Franke, H. Neumann, J. Hahn, M. Röder, and F. Richter, *Appl. Phys. Lett.* **70**, 1819 (1997).
- [19] M. I. Alonso and M. Garriga, *Thin Solid Films* **455/456**, 124 (2004).
- [20] C. M. Herzinger, P. G. Snyder, B. Johs, and J. A. Woollam, *J. Appl. Phys.* **77**, 1715 (1995).